Heat and mass transport behavior in bio-convective reactive flow of nanomaterials with Soret and Dufour characteristics.

KHAN, M.I., SHAH, F., ABDULLAEV, S.S., LI, S., ALTUIJRI, R., VAIDYA, H. and KHAN, A.

2023

Case Studies in Thermal Engineering 49 (2023) 103347

Contents lists available at ScienceDirect

Case Studies in Thermal Engineering

journal homepage: www.elsevier.com/locate/csite

Heat and mass transport behavior in bio-convective reactive flow of nanomaterials with Soret and Dufour characteristics

M. Ijaz Khan [a,b,c,*], Faisal Shah [d], Sherzod Shukhratovich Abdullaev [e,f], Shuguang Li [g], Reem Altuijri [h], Hanumesh Vaidya [i], Ashfaq Khan [j]

[a] Department of Mechanics and Engineering Science, Peking University, Beijing, 100871, China
[b] Department of Mechanical Engineering, Lebanese American University, Kraytem, Beirut, 1102-2801, Lebanon
[c] Department of Mathematics and Statistics, Riphah International University, I-14, Islamabad, 44000, Pakistan
[d] Research Center of Fluid Mechinery Engineering and Technology, Jiangsu University, Zhenjiang, 212013, China
[e] Faculty of Chemical Engineering, New Uzbekistan University, Tashkent, Uzbekistan
[f] Department of Science and Innovation, Tashkent State Pedagogical University named after Nizami, Bunyodkor Street 27, Tashkent, Uzbekistan
[g] School of Computer Science and Technology, Shandong Technology and Business University, Yantai, 264005, China
[h] Department of Physics, College of Science, Princess Nourah bint Abdulrahman University, P. O. Box 84428, Riyadh, 11671, Saudi Arabia
[i] Department of Mathematics, Vijayangara Sri Krishnadevaraya University, Ballari, Karnataka, India
[j] School of Engineering, Robert Gordon University, Aberdeen, AB10 7GJ, United Kingdom

ARTICLE INFO

Handling Editor: Huihe Qiu

Keywords:
Sutterby nanofluid
Bioconvection
Brownian movement
Thermal radiation
Heat generation and thermophoresis

ABSTRACT

The main of this article is to analyze magnetohydrodynamic bioconvective flow of Sutterby nanoliquid. Gyrotactic microorganism in presence of chemical reaction is addressed. Thermophoretic, magnetic field, random motion heat generation and radiation are discussed. Furthermore, Dufour and Soret behaviors are taken into account. Thermal conduction augmentation performance is discussed by utilization Boungiorno's model. Nonlinear PDE's (partial differential equations) are changed to ordinary system through appropriate variables. To developed computational solutions, we used the ND-solve technique. Results for temperature, microorganism field, liquid flow, and concentration are exhibited through different emerging variables. The physical quantities like Nusselt number, microorganism density number and solutal transport rate for various sundry variables are presented. Summary of main results re highlighted in the conclusions. Velocity reduces against magnetic field, while reverse trend seen for buoyancy ratio variable. Thermal distribution has an enhancing trend for magnetic and radiation variables. An enhancement in concentration distribution is seen for Soret number.

1. Introduction

Bioconvection is due to the up swimming of microorganisms caused due to density gradient and becomes unstable or destabilized. In the fluidic environment microorganisms display extensive versatility in swimming directions. The happening of bioconvection gives a modern way of mixing and controlling mass transport in diverse fluid flow problems. Bioconvection is a new kind of convection which is essential in biologic polymerization mixtures, ecosystem, oil recovery system and hydrogen fuel. Aziz et al. [1] studied the bioconvection flow of hybrid nanoliquid within presence of motile microorganism due to stretched porous medium. Solutal and thermal transfer analysis for bioconvective slip flow of nanoliquid towards stretching/shrinking medium is explained by Uddin et al.

* Corresponding author. Department of Mechanics and Engineering Science, Peking University, Beijing 100871, China.
E-mail address: scientificresearchglobe@gmail.com (M.I. Khan).

https://doi.org/10.1016/j.csite.2023.103347
Received 12 January 2023; Received in revised form 24 July 2023; Accepted 26 July 2023
Available online 27 July 2023

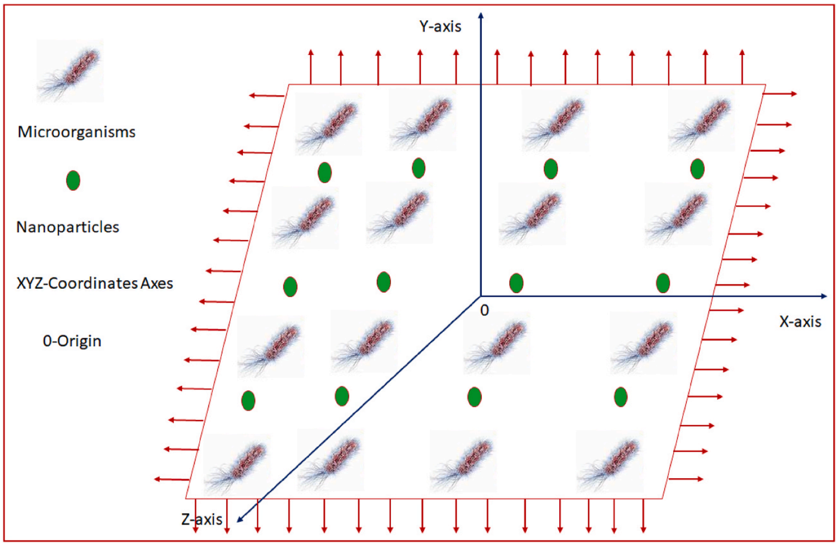

Fig. 1. Flow diagram.

[2]. Thermal transport analysis in bioconvective flow of nanoliquid considering motile microorganism is illustrated by Kuznetsov [3]. Bioconvection stratified magnetohydrodynamic flow of Oldroyd-B nanoliquid with microorganism field considering heat source due stretched wall is executed by Waqas et al. [4]. Performance of activation energy in bioconvection magnetized Williamson material in presence of radiation influence is examined by Asjad et al. [5]. Alsaedi et al. [6] reported the heat and solutal transfer rate analysis in bioconvection MHD flow of nanoliquid containing motile microorganisms. Zhang et al. [7] elaborated the hydromagnetic bio-convective flow of Williamson nanoliquid containing microorganism saturated in Darcy-Forchheimer medium. Recently, various researchers and investigators works on multiple innovative concept regarding interlayer exchange coupling [8], entropy optimized reactive flow with Ohmic heating [9], bio-inspired magnetism-responsive hybrid micro-structures [10], velocity slip flow with ternay nanofluid [11], first hidden charm penta-quark [12], bio-convective Maxwell fluid flow [13] and modeling of nano-graphite film and vapor-liquid equilibrium for electrolyte solutions [14,15].

Recently, nanofluids have been proven to be very effective as base fluid due to their remarkable thermophysical properties (density, thermal conductivity, viscosity and specific heat) in heat transfer rate. Nanofluids are fluids which contain nanometer sized particle. The nanoparticles are very small size same as to de Brogile or coherent wavelength. Because of this nanoparticles action like energy materials. Nanofluids are the homogeneous mixture of nanometer sized particles (1-100 nm) in a conventional fluid. Recent engineers and scientists have received much attention about nanoliquid due to essential thermal properties. An improvement of the thermal efficiency of their exchangers is one of the various application of this material. Nanoliquids having applications likes vehicle cooling, nanowires, nanofibers, cancer therapy, engine cooling, fuel cells, inorganic lungs, domestic refrigerator, pharmaceutical processes, electronic cooling system and radiators etc. Choi and Eastman [16 and 17] were the first who introduced the concept of nanofluids. Choi investigated thermal conductivity of nanomaterials. Afterwards many researchers explored the mechanisms of nanofluid in different geometrical domains. Due to a wide variety of applications in science and technology nanofluids have attained much attention by researchers and scientists. Nanofluids are primarily used in heat transfer equipment, in solar collectors, polymerase chain reaction and many others. After that Buongiorno [18] gave the theoretical model and described the seven-slip characteristics for heat transportation in nanoliquid. Reddy and Makinde [19] investigated buoyancy forces, thermophoretic and random movement for hydrodynamic Jeffrey nanoliquid flow. Irreversibility and radiation analysis for chemically reactive MHD nanoliquid flow is investigated by Khan et al. [20]. Variable viscosity impact in propylene glycol-based hybrid nanoliquid flow with heat generation is illuminated by Khan et al. [21]. Wang et al. [22], Zhang et al. [23] and Xiang et al. [24] highlight thermal evolution of chemical structure, advanced energy materials and directional fluid spreading on micro-fluidic chip structure respectively. Rasool et al. [25,26] numerically explored MHD Al_2O_3–Cu/engine oil based flow and EMHD non-Darcian flow towards a Riga surface. Khan et al. [27] and Li et al. [28,29] examined reactive based fluid flow with different flow geometries. Further discussions in this direction are given as follows: numerical solution for multi-layer granular bed filter [30], radiative flow for four different types of nanoparticles with non-uniform heat source [31], micropolar nanofluid flow through lid driven cavity [32], fluid flow analysis in the presence of chemical reaction [33,34], non-Darcian nano fluid flow and bio-convective processes for cross nanofluid [35,37] and Arrhenius activation energy impact in fluid flow [36,38].

Objective of recent analysis is to explore the bioconvective hydromagnetic Sutterby nanoliquid flow. Motile microorganism along with thermophoretic and random movement are addressed. Heat generation, magnetohydrodynamic effect and radiation are scrutinized in energy expression. Additionally, Soret and Dufour characteristics are taken into consideration. ND-solve technique is utilized to get numerical solutions for the given dimensionless expression. Outcomes of secondary variables on temperature, microorganism field, velocity and concentration are analyzed. Physical analysis of heat transfer rate, microorganism density number and solutal transfer rate versus flow variables are examined.

2. Formulation

Consider three-dimensional bioconvective magnetized flow of Sutterby nanomaterial. Buongiorno's model along with motile microorganism is addressed. Thermal radiation, magnetohydrodynamic effect and heat generation are taken into consideration. Furthermore, Soret and Dufour behaviors are taken into account. Magnetic field of strength (B_0) is applied. Surface is stretched bidirectional having velocities $u_w(=ax)$, $v_w(=by)$ with $a,\ b>0$. Fig. 1 presents flow diagram.

The related expressions are given by [39–42]:

$$\frac{\partial u}{\partial x}+\frac{\partial v}{\partial y}+\frac{\partial w}{\partial z}=0, \tag{1}$$

$$\left.\begin{aligned} &u\frac{\partial u}{\partial x}+v\frac{\partial u}{\partial y}+w\frac{\partial u}{\partial z}=\nu_f\frac{\partial^2 u}{\partial z^2}\left[1-\frac{\beta^2}{6}\left(\frac{\partial u}{\partial z}\right)^2\right]^n-\frac{n\nu_f\beta^2}{3}\left(\frac{\partial u}{\partial z}\right)^2\times\frac{\partial^2 u}{\partial z^2}\left[1-\frac{\beta^2}{6}\left(\frac{\partial u}{\partial z}\right)^2\right]^{n-1}\\ &-\frac{\sigma_f B_0^2}{\rho_f}u+\frac{1}{\rho_f}\left(\rho_f(1-C_\infty)(T-T_\infty)g\beta^*-\left(\rho_p-\rho_f\right)(C-C_\infty)g-\left(\rho_m-\rho_f\right)(N-N_\infty)g\gamma^*\right)\end{aligned}\right\}, \tag{2}$$

$$\left.\begin{aligned} &u\frac{\partial v}{\partial x}+v\frac{\partial v}{\partial y}+w\frac{\partial v}{\partial z}=\nu_f\frac{\partial^2 v}{\partial z^2}\left[1-\frac{\beta^2}{6}\left(\frac{\partial v}{\partial z}\right)^2\right]^n-\frac{n\nu_f\beta^2}{3}\left(\frac{\partial v}{\partial z}\right)^2\frac{\partial^2 v}{\partial z^2}\times\left[1-\frac{\beta^2}{6}\left(\frac{\partial v}{\partial z}\right)^2\right]^{n-1}\\ &-\frac{\sigma_f B_0^2}{\rho_f}v=0\end{aligned}\right\}, \tag{3}$$

$$\left.\begin{aligned} &u\frac{\partial T}{\partial x}+v\frac{\partial T}{\partial y}+w\frac{\partial T}{\partial z}=\alpha_f\frac{\partial^2 T}{\partial z^2}+\tau\left(D_B\frac{\partial C}{\partial z}\frac{\partial T}{\partial z}+\frac{D_T}{T_\infty}\left(\frac{\partial T}{\partial z}\right)^2\right)+\frac{\sigma_f B_0^2}{\rho_f}\left(u^2+v^2\right)\\ &+\frac{16\sigma^* T_\infty^3}{3k^*(\rho c_p)_f}\frac{\partial^2 T}{\partial z^2}+\frac{D_B k_T}{c_p C_s}\frac{\partial^2 C}{\partial z^2}+\frac{Q_0}{(\rho c_p)_f}(T-T_\infty)\end{aligned}\right\}, \tag{4}$$

$$u\frac{\partial C}{\partial x}+v\frac{\partial C}{\partial y}+w\frac{\partial C}{\partial z}=D_B\frac{\partial^2 C}{\partial z^2}+\frac{D_T}{T_\infty}\frac{\partial^2 T}{\partial z^2}+\frac{D_B k_T}{T_m}\frac{\partial^2 T}{\partial z^2}-k_r^2(C-C_\infty), \tag{5}$$

$$u\frac{\partial N}{\partial x}+v\frac{\partial N}{\partial y}+w\frac{\partial N}{\partial z}+\left(\frac{\partial}{\partial z}\left(N\frac{\partial C}{\partial z}\right)\right)\frac{b^* W_c}{(C_w-C_\infty)}=D_m\frac{\partial}{\partial z}\left(\frac{\partial N}{\partial z}\right) \tag{6}$$

With [39–42]:

$$\left.\begin{aligned} &u=U_w=ax, v=V_w=by, w=0, -k_f\frac{\partial T}{\partial z}=h_f(T_w-T),\ -D_B\frac{\partial C}{\partial z}=h_m(C_w-C), -D_m\frac{\partial N}{\partial z}=h_k(N_w-N)\quad \text{at } z=0\\ &u\to 0, v\to 0, T\to T_\infty, C\to C_\infty\ N\to N_\infty\ \ \text{as } z\to\infty\end{aligned}\right\}. \tag{7}$$

Here (u,v,w) denotes the velocity components, n power law index, (x,y,z) Cartesian coordinates, β material constant, k_T thermal diffusion ratio, Q_0 heat source coefficient, b^* chemo taxis constant, $(\rho c_p)_p$ effective heat capacity of nanoparticles, h_m mass transfer rate, β^* volume expansion coefficient, D_T thermophoresis coefficient, W_c cell swimming speed, T_w wall temperature, C_∞ ambient concentration, N_w wall microorganism concentration, C concentration, σ_f electrical conductivity, γ^* microorganism average volume, h_f heat transfer rate, β_0 magnetic field strength, h_k microorganism transfer rate, C_s concentration susceptibility, ρ_f density, α_f thermal diffusivity, g gravity, T temperature, N_∞ ambient microorganism concentration, k_f thermal conductivity, c_p specific heat, k_r reaction rate, T_∞ ambient temperature, T_m mean fluid temperature, σ^* Stefan-Boltzman constant, D_m swimming microorganism coefficient, ρ_m microorganism density, ρ_p nanoparticle density, $(\rho c_p)_f$ heat capacity of fluid, ν_f kinematic viscosity, C_w wall concentration, D_B Brownian motion coefficient, N microorganism concentration, k^* mean absorption coefficient and $\tau\left(=\frac{(\rho c_p)_p}{(\rho c_p)_f}\right)$ ratio of capacities.

Considering [43]:

$$\left.\begin{aligned} &u=axf'(\eta), v=ayg'(\eta), w=-\sqrt{a\nu}(f(\eta)+g(\eta)), \theta(\eta)=\frac{T-T_\infty}{T_w-T_\infty}\\ &\varphi(\eta)=\frac{C-C_\infty}{C_w-C_\infty}, \chi(\eta)=\frac{N-N_\infty}{N_w-N_\infty}, \eta=z\sqrt{\frac{a}{\nu_f}}\end{aligned}\right\}. \tag{8}$$

We have

Table 1
Nusselt number results comparison with Lone et al. [44].

Pr	Lone et al. [44]	Recent outcomes
0.72	0.463144	0.4631135
1.0	0.581976	0.5819757
3.0	1.165245	1.1652449
7.0	1.895403	1.8954046
10.0	2.308003	2.3080025

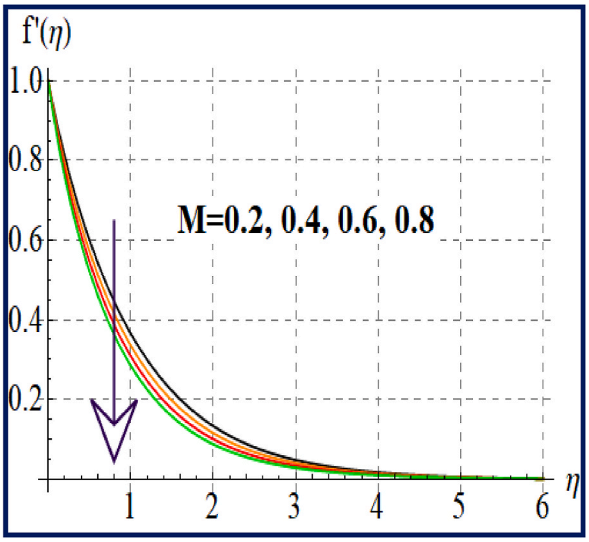

Fig. 2. $f^{'}(\eta)$ via M.

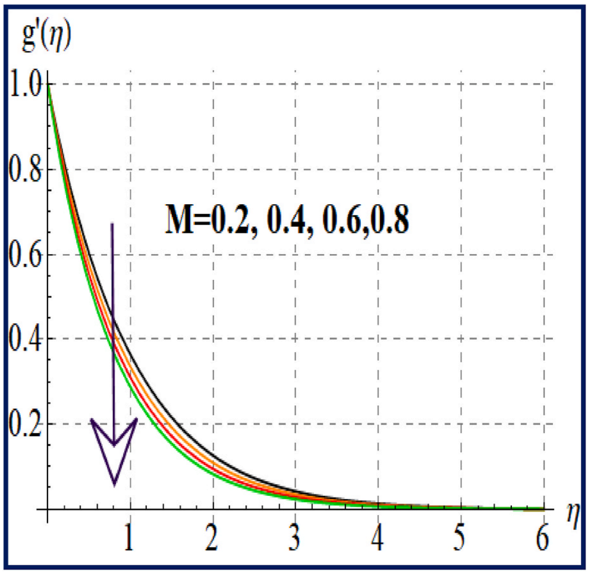

Fig. 3. $g^{'}(\eta)$ via M.

$$\left.\begin{array}{l}\left(1-\frac{\alpha_1}{6}f''^2\right)^n f''' - \frac{n\alpha_1}{3}\left(1-\frac{\alpha_1}{6}f''^2\right)^{n-1} f''^2 f''' + (f+g)f'' - f'^2 \\ \qquad +\lambda(\theta - N_r\varphi - R_b\chi) - Mf' = 0\end{array}\right\}, \tag{9}$$

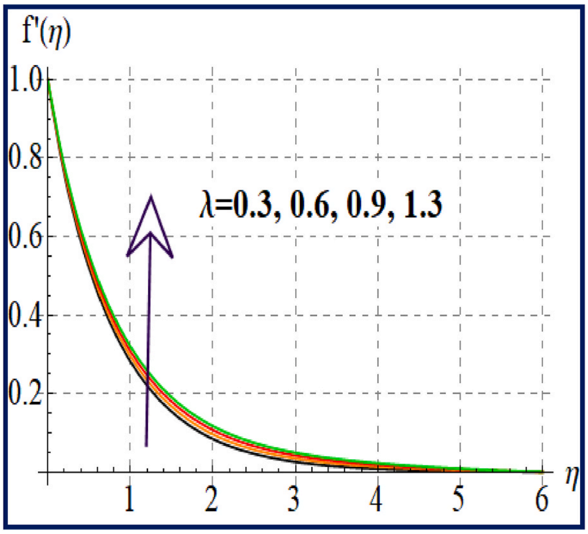

Fig. 4. $f'(\eta)$ via λ.

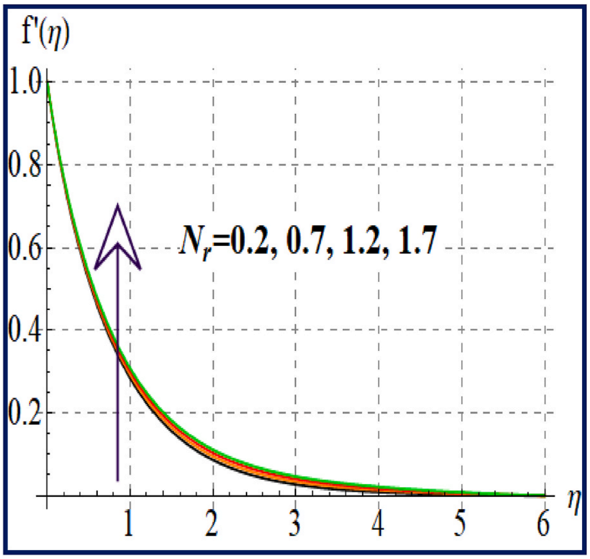

Fig. 5. $f'(\eta)$ via N_r.

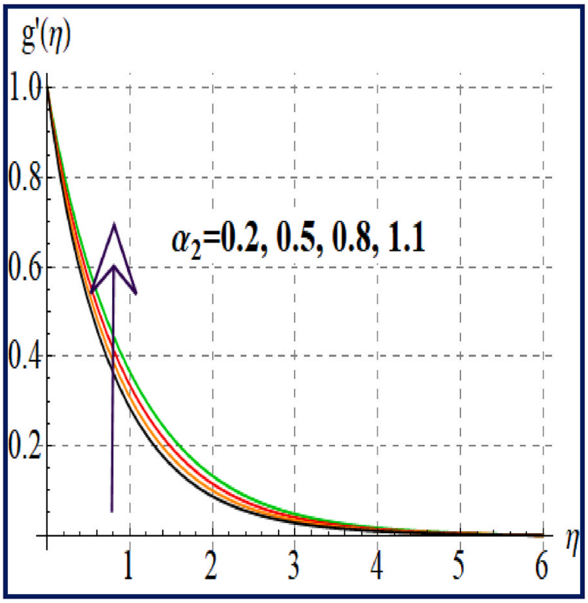

Fig. 6. $f'(\eta)$ via α_2.

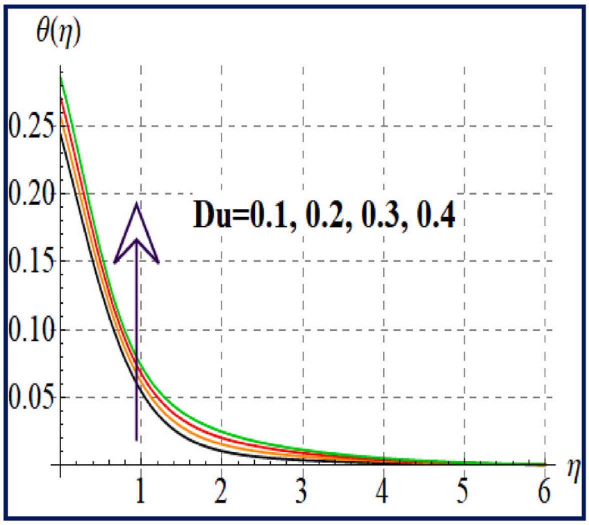

Fig. 7. $\theta(\eta)$ via Du.

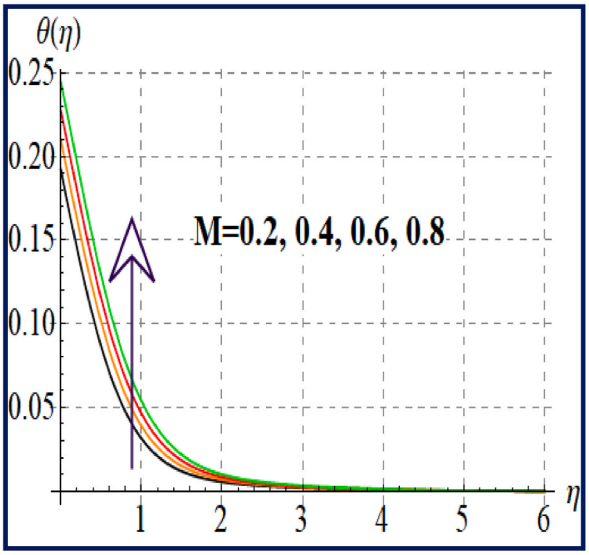

Fig. 8. $\theta(\eta)$ via M.

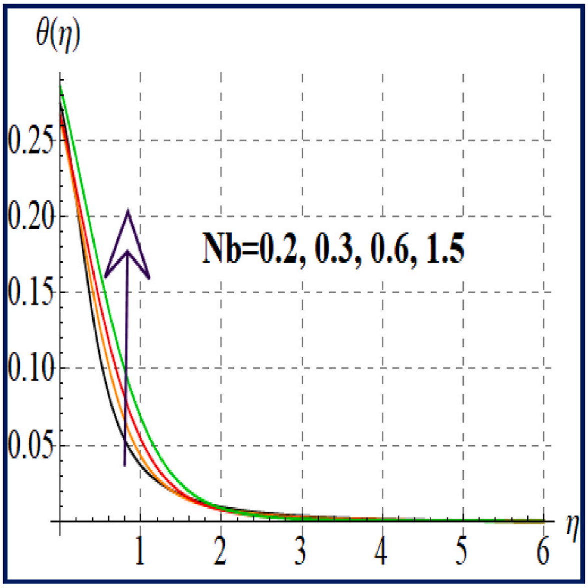

Fig. 9. $\theta(\eta)$ via Nb.

$$\left.\left(1-\frac{\alpha_2}{6}g''^2\right)^n g''' - \frac{n\alpha_2}{3}\left(1-\frac{\alpha_2}{6}g''^2\right)^{n-1} g''^2 g''' + (f+g)\,g'' - g'^2 - Mg' = 0\right\}, \tag{10}$$

$$\left.\begin{aligned}&(1+Rd)\,\theta'' + \Pr(f+g)\,\theta' - \Pr f\theta' + \Pr Du\varphi'' + M\Pr Ec\left(f'^2+g'^2\right)\\ &\Pr\left(Nb\theta'\varphi' + Nt\theta'^2 + Q\theta\right) = 0\end{aligned}\right\}, \tag{11}$$

$$\varphi'' + Le(f+g)\,\varphi' - f\varphi' + \frac{Nt}{Nb}\theta'' - \gamma Le\varphi + LeSr\theta'' = 0, \tag{12}$$

$$\chi'' + Lb(f+g)\,\chi' - Pe(\Omega\varphi'' + \chi\varphi'' + \varphi'\chi') = 0, \tag{13}$$

with

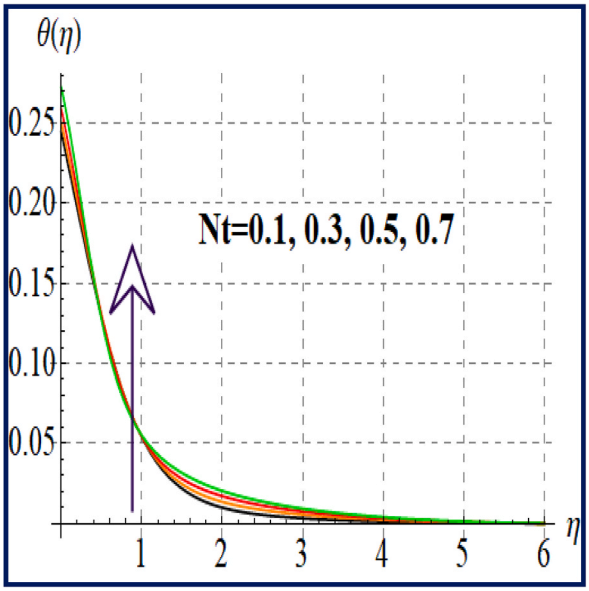

Fig. 10. $\theta(\eta)$ via Nt.

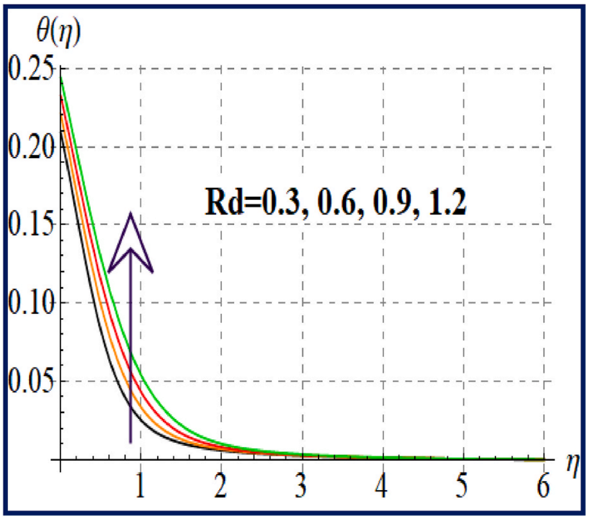

Fig. 11. $\theta(\eta)$ via Rd.

$$\left.\begin{array}{l} f'(0)=1, f(0)=0, g'(0)=\in, g(0)=0\ \theta'(0)=-\beta_1(1-\theta(0)), \\ \varphi'(0)=-\beta_2(1-\varphi(0)), \chi'(0)=-\beta_3(1-\chi(0)) \\ f'(\infty)=0, g'(\infty)=0, \theta(\infty)=0, \varphi(\infty)=0, \chi(\infty)=0 \end{array}\right\}. \tag{14}$$

Here $Rd\left(=\frac{16\sigma^* T_\infty^3}{3k^* k_f}\right)$ indicates the radiation variable, $Le\left(=\frac{\nu_f}{D_B}\right)$ the Lewis number, $\lambda\left(=\frac{g\beta^*(T_w-T_\infty)\,(1-C_\infty)}{a\rho_f}\right)$ the mixed convection variable, $\in\left(=\frac{b}{a}\right)$ the ratio parameter, $\alpha_1\left(=\frac{\beta^2 a^3 x^2}{\nu_f}\right)$ the material variable, $\beta_2\left(=\frac{h_m}{D_B}\sqrt{\frac{\nu_f}{a}}\right)$, solutal Biot number, $N_r\left(=\frac{(\rho_p-\rho_f)\,(C_w-C_\infty)}{\rho_f\beta^*(T_w-T_\infty)\,(1-C_\infty)}\right)$ the Buoyancy ratio parameter, $\beta_1\left(=\frac{h_f}{k_f}\sqrt{\frac{\nu_f}{a}}\right)$, thermal Biot number, $R_b\left(=\frac{(\rho_m-\rho_f)\,(N_w-N_\infty)\,\gamma^*}{\rho_f(T_w-T_\infty)\,(1-C_\infty)\,\beta^*}\right)$ the bioconvective Rayleigh number, $Lb\left(=\frac{\nu_f}{D_m}\right)$ the bioconvective Lewis number, $M\left(=\frac{\sigma_f B_0^2}{a\rho_f}\right)$ the magnetic variable, $Pe\left(=\frac{bW_c}{D_m}\right)$ the Peclet number, $Q\left(=\frac{Q_0}{a(\rho c_p)_f}\right)$ the heat generation variable, $\Pr\left(=\frac{\nu_f}{\alpha_f}\right)$ the Prandtl number, $\alpha_2\left(=\frac{\beta^2 a^3 y^2}{\nu_f}\right)$ the material variable, $\gamma\left(=\frac{k_r}{a}\right)$ the reaction variable, $\beta_3\left(=\frac{h_k}{D_m}\sqrt{\frac{\nu_f}{a}}\right)$ microorganism Biot number, $Ec\left(=\frac{(ax)^2}{(c_p)_f(T_w-T_\infty)}\right)$ the Eckert number, $Nt\left(=\frac{\tau D_T(T_w-T_\infty)}{\nu_f T_\infty}\right)$, the thermophoresis parameter, $Nb\Big(=$

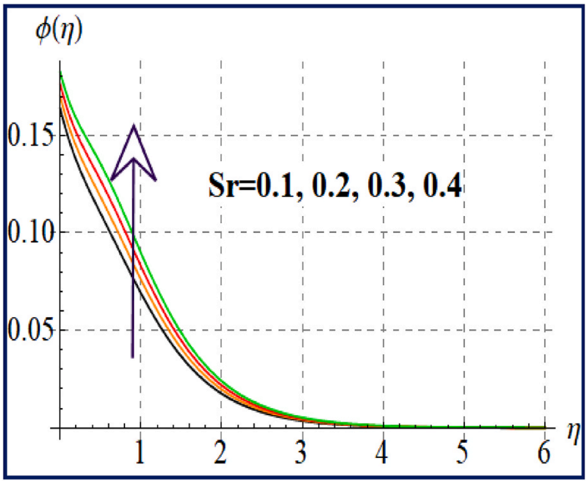

Fig. 12. $\varphi(\eta)$ via *Sr*.

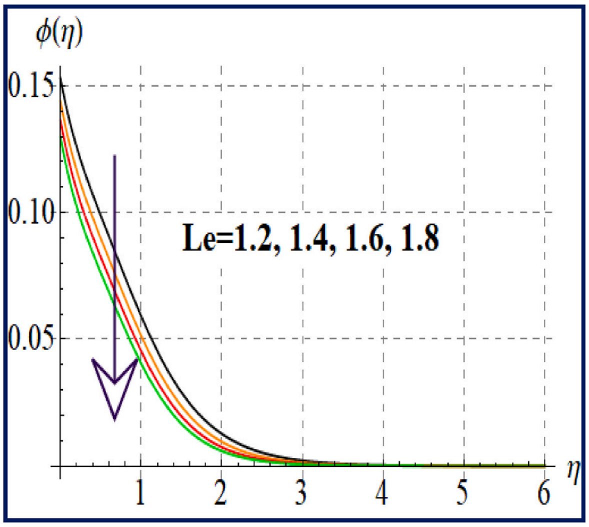

Fig. 13. $\varphi(\eta)$ via *Le*.

$\frac{\tau D_B(C_w - C_\infty)}{\nu_f}\Big)$, the Brownian motion parameter and $\Omega\left(=\frac{N_\infty}{(N_w - N_\infty)}\right)$ the microorganism difference parameter.

3. Quantities of interest

3.1. Nusselt number

Mathematically it is

$$Nu_x = \frac{xq_w}{k_f(T_w - T_\infty)}, \tag{15}$$

q_w heat flux satisfies

$$q_w = -\left(k_f + \frac{16\sigma^* T_\infty^3}{3k^*}\right)\left(\frac{\partial T}{\partial z}\right)\bigg|_{z=0}, \tag{16}$$

Dimensionless equation is

$$Nu_x \mathrm{Re}_x^{-1/2} = -(1 + Rd)\,\theta'(0). \tag{17}$$

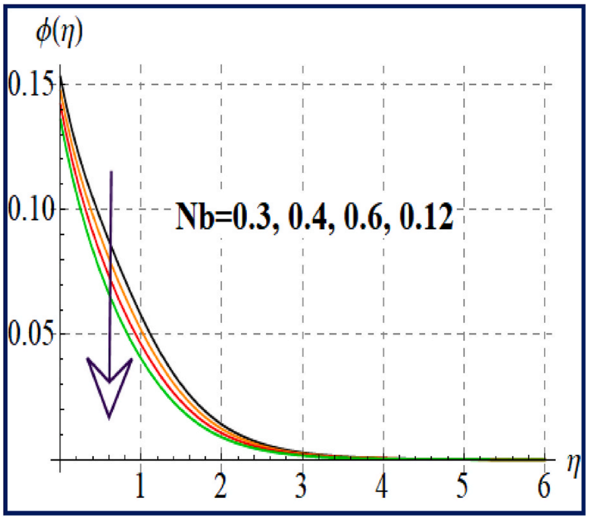

Fig. 14. $\varphi(\eta)$ via *Nb*.

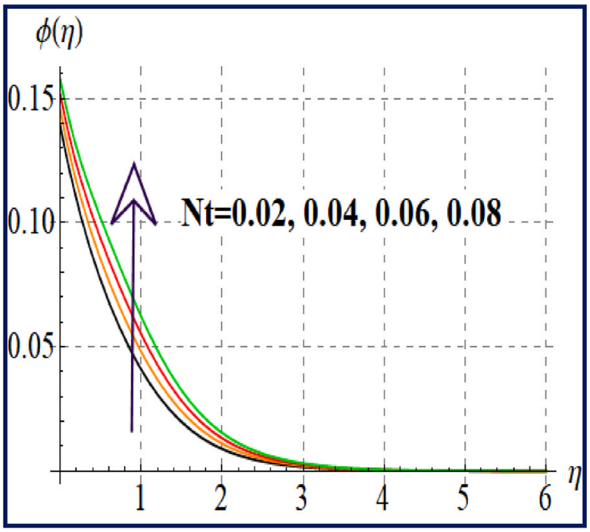

Fig. 15. $\varphi(\eta)$ via *Nt*.

3.2. Sherwood number

It is expressed as

$$Sh_x = \frac{x j_w|_{z=0}}{D_B(C_w - C_\infty)}, \tag{18}$$

here j_w mass flux is defined as

$$j_w = -D_B\left(\frac{\partial C}{\partial z}\right), \tag{19}$$

We get

$$Sh_x \mathrm{Re}_x^{-1/2} = -\varphi'(0). \tag{20}$$

3.3. Microorganisms density number

It is given as

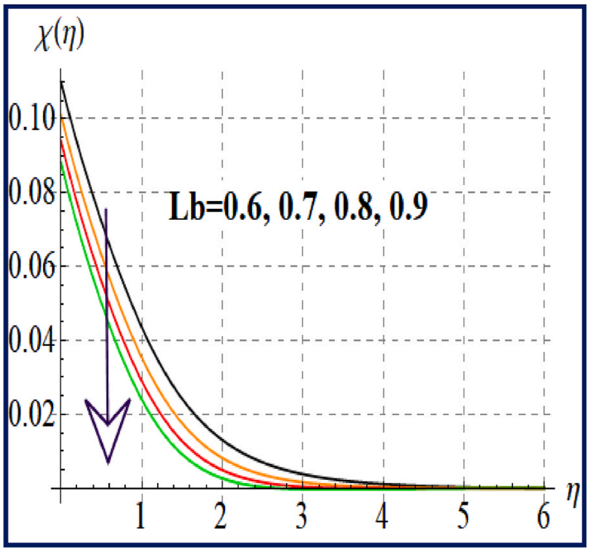

Fig. 16. $\chi(\eta)$ via *Lb*.

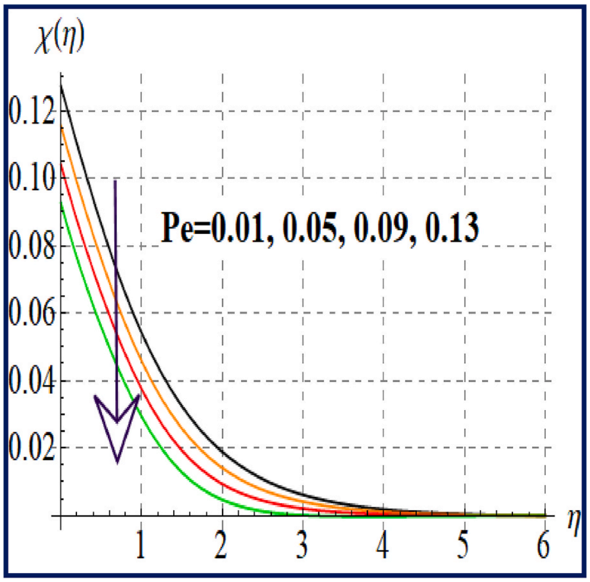

Fig. 17. $\chi(\eta)$ via *Pe*.

$$Sn_x = \frac{xj_n|_{z=0}}{D_m(N_w - N_\infty)}, \tag{21}$$

in which j_n microorganism flux is

$$j_n = -D_m\left(\frac{\partial N}{\partial z}\right). \tag{22}$$

One can found

$$Sn_x \mathrm{Re}_x^{-1/2} = -\chi'(0). \tag{23}$$

In above equations $\mathrm{Re}_x = \frac{ax^2}{\nu_f}$ represents the local Reynolds number.

Table 2
Results for thermal transport rate.

Nt	*Nb*	*Rd*	Nu_x
0.1	0.2	1.2	0.589609
0.3			0.584711
0.5			0.578188
0.7			0.56769
0.8	0.2	1.2	0.565881
	0.3		0.574718
	0.4		0.574501
	0.5		0.57325
0.1	0.2	0.3	0.332234
		0.6	0.420791
		0.9	0.506546
		1.2	0.589609

Table 3
Numerical outcomes for solutal transfer rate.

Sr	*Nt*	*Nb*	Sh_x
0.1	0.1	0.2	0.167237
0.2			0.165988
0.3			0.164744
0.4			0.163503
0.1	0.02	0.2	0.172212
	0.4		0.170944
	0.06		0.169691
	0.08		0.168455
0.1	0.3	0.1	0.169406
	0.6		0.170502
	0.6		0.171619
	1.2		0.172819

Table 4
Computational outcomes for microorganism density number.

Lb	*Pe*	Sn_x
0.6	0.1	0.0890018
0.7		0.0898872
0.8		0.0905972
0.9		0.0911799
0.7	0.01	0.0872824
	0.05	0.0884499
	0.09	0.0896017
	0.13	0.090738

4. Discussion

This section is organized for discussions of liquid flow, microorganism field, temperature, physical quantities and concentration. Comparison analysis of recent investigations with previous published analysis of Lone et al. [44] is mentioned in Table 1. Clearly one can found that both results are in an excellent agreement.

4.1. Velocity

Figs. (2 and 3) illustrates the flow ($f'(\eta), g'(\eta)$) variation for magnetic field. Higher magnetic field induces more disturbance in flow region and the velocities ($f'(\eta), g'(\eta)$) declined. Variation of (λ) on velocity is disclosed in Fig. 4. Clearly the fluid flow ($f'(\eta)$) is noticed an increasing function of mixed convection variable. Fig. 5 elucidates the behavior of ($f'(\eta)$) against buoyancy ratio variable. An increment in velocity is seen for larger estimation of buoyancy ratio variable. Fig. 6 sketched to show velocity ($g'(\eta)$) impact (α_2). Higher approximation of (α_2) corresponds to upsurges the velocity field.

4.2. Temperature

Feature of Dufour number on ($\theta(\eta)$) is exhibited in Fig. 7. An increase in thermal distribution is detected via higher estimation of Dufour (*Du*) number. Fig. 8 depicts ($\theta(\eta)$) against (*M*). With higher (*M*) the resistive forces induce more resistance the flow system. As a result, the temperature upsurges. Figs. (9 and 10) are displayed to examine thermal ($\theta(\eta)$) distribution for random (*Nb*) and thermophoresis (*Nt*) variables. Clearly one can detected that thermal ($\theta(\eta)$) field upsurges for both random (*Nb*) and thermophoresis (*Nt*) diffusion variables. Fig. 11 depicts the magnification in $(\theta(\eta))$ with increasing (Rd). Clearly higher radiation (Rd) results into creation of more heat inside system which cause increase in temperature.

4.3. Concentration

The action of $(\varphi(\eta))$ through (Sr) is depicted in Fig. 12. As anticipated the Concentration $(\varphi(\eta))$ distribution is boosted via larger Soret (Sr) number. Fig. 13 indicates $(\varphi(\eta))$ variation via (Le). Physically Lewis number has inverse relation with mass diffusivity. So far big Lewis number the liquid has small mass diffusivity, as a consequence $(\varphi(\eta))$ decreases. Concentration field behavior subject to random (Nb) and thermophoresis (Nt) variables are disposed in Figs. (14 and 15). An increase in concentration has been detected for higher values of (Nt), while reverse impact occurs for (Nb).

4.4. Microorganism field

Trend of $(\chi(\eta))$ for higher bioconvection Lewis number is shown in Fig. 16. The microorganism $(\chi(\eta))$ field is decayed for larger values of (Lb). The action of $(\chi(\eta))$ through Peclet (Pe) number is shown in Fig. 17. Clearly a reduction occurs in microorganism $(\chi(\eta))$ field for larger values of Peclet (Pe) number.

4.5. Engineering quantities

Here heat transfer rate (Nu_x) microorganism density number (Sn_x) and solutal transport rate (Sh_x) are discussed.

4.5.1. Thermal transport rate

Variation of influential variables (like Nt, Nb and Rd) on (Nu_x) is mentioned in Table 2. A reduction in heat transport (Nu_x) rate is witnessed for higher (Nt) and (Nb). The Nusselt (Nu_x) number is boosted with increasing radiation variable.

4.5.2. Mass transport rate

Impact of Soret (Sr) number, random (Nb) and thermophoretic (Nt) variable is highlighted in Table 3. Obviously (Sh_x) is improved versus random (Nb) variable. Solutal transport (Sh_x) rate decrement is detected for higher (Nt) and (Nb).

4.5.3. Microorganisms density number

Microorganism density (Sn_x) number variation against (Lb) and (Pe) is mentioned in Table 4. There is an increase in (Sn_x) occurs for Peclet number. Microorganism density number (Sn_x) enhancement is noticed for bioconvection Lewis number.

5. Closing remarks

The following main results are mentioned:

Decreasing impact for velocities $(f'(\eta), g'(\eta))$ occurs through magnetic field.

- Increase in flow is detected for buoyancy ratio variable.
- The velocity is boosted against mixed convection variable.
- Increase in temperature is noticed for Dufour (Du) number and magnetic (M) field.
- Thermal distribution improves via larger values of thermophoresis (Nt) and random (Nb) motion variables.
- Radiation effect leads to upsurges thermal distribution and Nusselt number.
- Decreasing in heat transport rate is detected for increasing values of (Nt) and (Nb).
- Lewis number leads to reduce concentration.
- Concentration for (Nt) and (Nb) has reverse impacts.
- An increment in concentration occurs for Soret number.
- Reverse trend in solutal transport rate is noticed for random (Nb) and thermophoresis (Nt) variables.
- Soret number variation decays mass transport rate.
- Peclet number leads to intensifies the microorganism density number, while opposite trend seen for microorganism field.
- Microorganisms field decays for larger bioconvection Lewis number,
- An increase in microorganism density number is detected for higher bioconvection (Lb) Lewis number.

Author contributions

All authors are equally contributed in the research work.

Declaration of competing interest

The authors declared that they have no conflict of interest and the paper presents their own work which does not been infringe any third-party rights, especially authorship of any part of the article is an original contribution, not published before and not being under consideration for publication elsewhere.

Data availability

No data was used for the research described in the article.

Acknowledgments

Princess Nourah bint Abdulrahman University Researchers Supporting Project number (PNURSP2023R399), Princess Nourah bint Abdulrahman University, Riyadh, Saudi Arabia.

References

[1] A. Aziz, W.A. Khan, I. Pop, Free convection boundary layer flow past a horizontal flat plate embedded in porous medium filled by nanofluid containing gyrotactic microorganisms, Int. J. Therm. Sci. 56 (2012) 48–57.
[2] M.J. Uddin, M.N. Kabir, O.A. Bég, Computational investigation of Stefan blowing and multiple-slip effects on buoyancy-driven bioconvection nanofluid flow with microorganisms, Int. J. Heat Mass Tran. 95 (2016) 116–130.
[3] A.V. Kuznetsov, The onset of nanofluid bioconvection in a suspension containing both nanoparticles and gyrotactic microorganisms, Int. Commun. Heat Mass Tran. 37 (2010) 1421–1425.
[4] M. Waqas, T. Hayat, S.A. Shehzad, A. Alsaedi, Transport of magnetohydrodynamic nanomaterial in a stratified medium considering gyrotactic microorganisms, Phys. B: Condens 529 (2018) 33–40.
[5] M.I. Asjad, M. Zahid, M. Inc, D. Baleanu, B. Almohsen, Impact of activation energy and MHD on Williamson fluid flow in the presence of bioconvection, Alex. Eng. J. 61 (2022) 8715–8727.
[6] A. Alsaedi, M.I. Khan, M. Farooq, N. Gull, T. Hayat, Magnetohydrodynamic (MHD) stratified bioconvective flow of nanofluid due to gyrotactic microorganisms, Adv. Powder Technol. 28 (2017) 288–298.
[7] X. Zhang, D. Yang, M.I.U. Rehman, A.A. Mousa, A. Hamid, Numerical simulation of bioconvection radiative flow of Williamson nanofluid past a vertical stretching cylinder with activation energy and swimming microorganisms, Case Stud. Therm. Eng. 33 (2022), https://doi.org/10.1016/j.csite.2022.101977.
[8] X. Fan, G. Wei, X. Lin, X. Wang, Z. Si, X. Zhang, W. Zhao, Reversible switching of interlayer exchange coupling through atomically thin VO2 via electronic state modulation, Matter 2 (6) (2020) 1582–1593.
[9] S. Li, M.I. Khan, F. Alzahrani, S.M. Eldin, Heat and mass transport analysis in radiative time dependent flow in the presence of Ohmic heating and chemical reaction, viscous dissipation: an entropy modeling, Case Stud. Therm. Eng. 42 (2023), 102722.
[10] Y. Bian, S. Zhu, X. Li, Y. Tao, C. Nian, C. Zhang, D. Wu, Bioinspired magnetism-responsive hybrid microstructures with dynamic switching toward liquid droplet rolling states, Nanoscale (2023), https://doi.org/10.1039/D3NR02082G.
[11] S. Li, V. Puneeth, A.M. Saeed, A. Singhal, F.A.M. Al-Yarimi, M.I. Khan, S.M. Eldin, Analysis of the Thomson and Troian velocity slip for the flow of ternary nanofluid past a stretching sheet, Sci. Rep. 13 (2023) 2340.
[12] H. Chen, W. Chen, X. Liu, X. Liu, Establishing the first hidden-charm pentaquark with strangeness, The Europ. Phys. J. C 81 (2021) 409.
[13] Z. Liu S. Li, T. Sadaf, S.U. Khan, F. Alzahrani, M.I. Khan, S.M. Eldin, Numerical bio-convective assessment for rate type nanofluid influenced by Nield thermal constraints and distinct slip features, Case Stud. Therm. Eng. 44 (2023), 102821.
[14] S. Du, J. Yin, H. Xie, Y. Sun, T. Fang, Y. Wang, R. Zheng, Auger scattering dynamic of photo-excited hot carriers in nano-graphite film, Appl. Phys. Lett. 121 (2022), 181104.
[15] W. Liu, C. Zhao, Y. Zhou, X. Xu, R.A. Rakkesh, Modeling of vapor-liquid equilibrium for electrolyte solutions based on COSMO-RS interaction, J. Chem. (2022), 9070055.
[16] A.S.M. Aljaloud, L. Manai, I. Tlili, Bioconvection flow of Cross nanofluid due to cylinder with activation energy and second order slip features, Case Stud. Therm. Eng. 42 (2023), https://doi.org/10.1016/j.csite.2023.102767.
[17] S.U.S. Choi, Enhancing thermal conductivity of fluids with nanoparticles, ASME J. Fluids Eng. Pub. Fed 231 (1995) 99–106.
[18] J.A. Eastman, S.U.S. Choi, S. Li, W. Yu, L.J. Thompson, Anomalously increased effective thermal conductivities of ethylene glycol-based nanofluids containing copper nanoparticles, Appl. Phys. Lett. 78 (2001) 718–720.
[19] J. Buongiorno, Convective transport in nanofluids, ASME J. Heat Transf. 128 (2006) 240–250.
[20] M.G. Reddy, O.D. Makinde, Magnetohydrodynamic peristaltic transport of Jeffrey nanofluid in an asymmetric channel, J. Mol. Liq. 223 (2016) 1242–1248.
[21] S.A. Khan, T. Hayat, A. Alsaedi, B. Ahmad, Melting heat transportation in radiative flow of nanomaterials with irreversibility analysis, Renew. Sustain. Energy Rev. 140 (2021), https://doi.org/10.1016/j.rser.2021.110739.
[22] Z. Wang, Q. Wang, C. Jia, J. Bai, Thermal evolution of chemical structure and mechanism of oil sands bitumen, Energy 244 (2022), 123190.
[23] X. Zhang, Y. Tang, F. Zhang, C. Lee, A novel aluminum-graphite dual-ion battery, Adv. Energy Mater. 6 (2016), 1502588.
[24] J. Xiang, J. Liao, Z. Zhu, P. Li, Z. Chen, J. Huang, X. Chen, Directional fluid spreading on microfluidic chip structured with microwedge array, Phys. Fluids 35 (2023), 62005.
[25] G. Rasool, A. Shafiq, X. Wang, A.J. Chamkha, A. Wakif, Numerical treatment of MHD Al2O3–Cu/engine oil-based nanofluid flow in a Darcy–Forchheimer medium: application of radiative heat and mass transfer laws, Int J Mod Phys B, Apr. (2023), https://doi.org/10.1142/S0217979224501297.
[26] G. Rasool, A. Wakif, X. Wang, A. Shafiq, A.J. Chamkha, Numerical passive control of alumina nanoparticles in purely aquatic medium featuring EMHD driven non-Darcian nanofluid flow over convective Riga surface, Alex. Eng. J. 68 (2023), https://doi.org/10.1016/j.aej.2022.12.032.
[27] M.I. Khan, S.A. Khan, T. Hayat, M.I. Khan, A. Alsaedi, Entropy optimization analysis in MHD nanomaterials (TiO2-GO) flow with homogeneous and heterogeneous reactions, Comput. Methods Progr. Biomed. 184 (2020), https://doi.org/10.1016/j.cmpb.2019.105111.
[28] S. Li, M.I. Khan, M. Rafiq, S.A.M. Abdelmohsen, S.S. Abdullaev, M.S. Amjad, Optimized framework for Darcy-Forchheimer flow with chemical reaction in the presence of Soret and Dufour effects: a shooting technique, Chem, Phys. Lett. 825 (2023), https://doi.org/10.1016/j.cplett.2023.140578.
[29] S. Li, K. Raghunath, A. Alfaleh, F. Ali, A. Zaib, M.I. Khan, S.M. Eldin, V. Puneeth, Effects of activation energy and chemical reaction on unsteady MHD dissipative Darcy-forcheimer squeezed flow of Casson fluid over horizontal channel, Sci. Rep. 13 (2023) 2666.
[30] H. Ding, S. Liang, L. Tong, S. Yin, L. Wang, Y. Ding, Numerical simulation of a multilayer granular bed filter: effect of bed structure on the filtration characteristics of high-temperature particulate matter, Powder Technol. 426 (2023), https://doi.org/10.1016/j.powtec.2023.118632.
[31] Y.M. Chu, M.I. Khan, T. Abbas, M.O. Sidi, K.A.M. Alharbi, U.F. Alqsair, S.U. Khan, M.R. Khan, M.Y. Malik, Radiative thermal analysis for four types of hybrid nanoparticles subject to non-uniform heat source: keller box numerical approach, Case Stud. Therm. Eng. 40 (2022), 102474.
[32] S. Batool, G. Rasool, N. Alshammari, I. Khan, H. Kaneez, N. Hamadneh, Numerical analysis of heat and mass transfer in micropolar nanofluids flow through lid driven cavity: finite volume approach, Case Stud. Therm. Eng. 37 (2022), https://doi.org/10.1016/j.csite.2022.102233.
[33] N.V. Ganesh, R. Kalaivanan, Q.M.A. Mdallal, K. Reena, Buoyancy driven second grade nano boundary layers over a catalytic surface with reaction rate, heat of reaction and activation energy at boundary, Case Stud. Therm. Eng. 28 (2021), https://doi.org/10.1016/j.csite.2021.101346.
[34] N.V. Ganesh, Q.M.A. Mdallal, R. Kalaivanan, K. Reena, Arrhenius kinetics driven nonlinear mixed convection flow of Casson liquid over a stretching surface in a Darcian porous medium, Heliyon 9 (2023), https://doi.org/10.1016/j.heliyon.2023.e16135.
[35] G. Rasool, A. Wakif, X. Wang, A. Shafiq, A.J. Chamkha, Numerical passive control of alumina nanoparticles in purely aquatic medium featuring EMHD driven non-Darcian nanofluid flow over convective Riga surface, Alex. Eng. J. 68 (2023) 747–762.
[36] R. Kalaivanan, N.V. Ganesh, Q.M.A. Mdallal, Buoyancy driven flow of a second-grade nanofluid flow taking into account the Arrhenius activation energy and elastic deformation: models and numerical results, Fluid Dynam. Mater. Process. 17 (2021) 319–332.
[37] G. Rasool, S.Z.H. Shah, T. Sajid, W. Jamshed, G.C. Altamirano, B. Keswani, R.A.S. Núñez, M.S. Chero, Spectral relaxation methodology for chemical and bioconvection processes for cross nanofluid flowing around an oblique cylinder with a slanted magnetic field effect, Coatings 12 (2022), https://doi.org/10.3390/coatings12101560.
[38] R. Kalaivanan, N. V Ganesh, Q.M.A. Mdallal, An investigation on Arrhenius activation energy of second grade nanofluid flow with active and passive control of nanomaterials, Case Stud. Therm. Eng. 22 (2020), https://doi.org/10.1016/j.csite.2020.100774.

[39] Z. Hussain, W.A. Khan, T. Muhammad, H.A. Alghamdi, M. Ali, M. Waqas, Dynamics of gyrotactic microorganisms for chemically reactive magnetized 3D Sutterby nanofluid flow comprising non-uniform heat sink-source aspects, J. Magn. Magn Mater. 578 (2023), https://doi.org/10.1016/j.jmmm.2023.170798.
[40] M.U. Rahman, T. Hayat, S.A. Khan, A. Alsaedi, Entropy generation in Sutterby nanomaterials flow due to rotating disk with radiation and magnetic effects, Math. Comput. Simulat. 197 (2022) 151–165.
[41] M.I.U. Rehman, H. Chen, A. Hamid, W. Jamshed, M.R. Eid, S.M.E. Din, H.A.E.W. Khalifa, A.A. Elmonem, Effect of Cattaneo-Christov heat flux case on Darcy-Forchheimer flowing of Sutterby nanofluid with chemical reactive and thermal radiative impacts, Case Stud. Therm. Eng. 42 (2023), https://doi.org/10.1016/j.csite.2023.102737.
[42] S. Li, M.I. Khan, A.B. Alruqi, S.U. Khan, S.S. Abdullaev, B.M. Fadhl, B.M. Makhdoum, Entropy optimized flow of Sutterby nanomaterial subject to porous medium: Buongiorno nanofluid model, Heliyon 9 (2023), https://doi.org/10.1016/j.heliyon.2023.e17784.
[43] T. Hayat, S.A. Khan, A. Alsaedi, Entropy analysis for second grade nanomaterials flow with thermophoresis and Brownian diffusions, Int. Commun. Heat Mass Tran. 127 (2021), https://doi.org/10.1016/j.icheatmasstransfer.2021.105564.
[44] S.A. Lone, M.D. Shamshuddin, S. Shahab, S. Iftikhar, A. Saeed, A.M. Galal, Computational analysis of MHD driven bioconvective flow of hybrid Casson nanofluid past a permeable exponential stretching sheet with thermophoresis and Brownian motion effects, J. Magn. Magn Mater. 580 (2023), https://doi.org/10.1016/j.jmmm.2023.170959.